Suppression of Self-Induced Depolarization
of High-Power Laser Radiation in Glass-Based Faraday Isolators

Efim Khazanov, Nikolay Andreev, Alexey Babin, Alexander Kiselev, and Oleg Palashov

Institute of Applied Physics, 46 Uljanov str., N.Novgorod, 603600 Russia

David H. Reitze

Physics Department, University of Florida, Gainesville, Florida, 32601

ABSTRACT

Light absorption in optical elements of Faraday rotators results in a non-uniform cross-sectional temperature distribution which leads to depolarization of laser radiation and, consequently, limits the isolation ratio of optical Faraday isolators. We show experimentally that the influence of the temperature dependence of the Verdet constant on the isolation ratio is negligibly small when compared with the influence of the photoelastic effect. We also present two novel methods of optical isolation which significantly reduce the depolarization caused by the photoelastic effect and increase the isolation ratio by two orders of magnitude in comparison with the conventional method. Our results confirm the possibility of magneto-optical glass-based Faraday isolators with isolation ratios of 30 dB for average laser powers of hundreds of watts.

OCIS codes: 140.6810, 230.3240, 230.5440

Over the past few years, the average power of continuous wave and repetitively pulsed lasers has significantly increased due to advances in laser materials, pumping methods, and thermal management [1,2]. Investigations of thermal effects caused by absorption of laser radiation in optical elements is therefore becoming more important. A Faraday isolator is one of the optical elements most influenced by parasitic thermal effects, since absorption coefficients in magneto-optical media are relatively high, on the order of 10^{-3} cm^{-1}. Absorption in optical elements of Faraday rotators results in a non-uniform cross-section distribution of temperature, which influences propagating laser radiation in three ways. First, transverse wavefront distortions are induced (thermal lensing) by the dependence of the refractive index on temperature [3]. Second, a non-uniform distribution of the rotation angle of the polarization plane is caused by the temperature dependence of Verdet constant [4]. Finally, the simultaneous appearance of circular birefringence (Faraday effect) and linear birefringence results from mechanical strains (photoelastic effect [5]) caused by temperature gradient.

Thermal lensing has almost no effect on polarization if the focal length of the thermal lens is much more than the length of the magneto-optical element (almost always so in practice). The second and the third mechanisms alter the polarization of a laser beam transmitted through a magneto-optical medium and, consequently, affect the isolation ratio of Faraday isolators. The resulting decrease in average power was studied in Ref. [6] where it was predicted that the influence of the temperature dependence of the Verdet constant can be neglected in comparison with the influence of the photoelastic effect. In ref. [7] two novel schemes of Faraday isolators were suggested and theoretically investigated, in which

2

the influence of the photoelastic effect on the depolarization ratio was significantly reduced. The purpose of the present work is twofold. First, we experimentally confirm the theoretical predictions in ref. [6], which show that the photoelastic effect limits the isolation ratio in Faraday isolators operating at high average powers of laser radiation. Second, we determine the efficiency of the novel configurations suggested in ref. [7] for compensating the photoelastic induced depolarization.

The basic idea of compensating depolarization consists of using two 22.5° rotators and a reciprocal optical element between them instead of one 45° Faraday rotator. In such a configuration, polarization distortions which a beam experiences while passing the first rotator, will be partially compensated in the second. Fig. 1 exhibits the traditional method of Faraday isolation (Fig. 1a) and two novel configurations for compensation of polarization distortions (Fig. 1b,c). In all of these methods, in the absence of thermal effects, a laser beam remains horizontally polarized after propagation through the Faraday rotator (from left to right) and passes through polarizer 4. When passing backward through the Faraday rotator, the laser beam becomes vertically polarized and is reflected by polarizer 1. The absorption-induced depolarization in the Faraday rotators leads to the horizontally polarized radiation that passes through polarizer 1. In the geometry shown in Fig. 1b, a $\lambda/2$ plate 6 whose optical axis is inclined counterclockwise at 22.5° is situated between two magneto-optical rotators 5,7, rotating polarization in opposite directions. An additional advantage of this method is alternating polarities of magnet field, which permits the maximation of isolation ratio [8]. A similar technique has recently been reported for compensating birefringence in Nd:YAG rods in double-pass design [9]. In the scheme shown in Fig. 1c,

between the magneto-optical rotators 5, rotating polarization in one direction, there is a reciprocal quartz polarization rotator 8, that rotates polarization at an angle 67.5° in the same direction (for the reverse pass) as the magneto-optical rotators. The depolarization ratio γ in all three geometries is given by

$$\gamma = P_t/(P_t + P_r) \tag{1}$$

where $P_{t,r}$ are the powers of laser beams transmitted and reflected by polarizer 1 (Fig. 1). In ref. [7] it was demonstrated that for glass elements the depolarization ratio in each arrangement is determined only by parameter p

$$p = \frac{P_h Q}{\lambda \kappa} \tag{2}$$

where Q is the thermo-optical constant [10] given by

$$Q = \left(\frac{1}{L}\frac{dL}{dT}\right)\frac{n_0^3}{4}\frac{1+\nu}{1-\nu}(p_{11} - p_{12}) \tag{3}$$

where L is glass length, ν is the Poison's ratio, $p_{i,j}$ are the photoelastic coefficients, κ is the thermal conductivity, n_o is the refraction index, P_h is the power released as heat in optical elements, and λ is a wavelength in vacuum. Here we assume that the beam is Gaussian and the absorption is independent on polarization state of the beam. It is important that the parameter p be equal for the both magneto-optical elements for optimal performance of the methods shown in Fig. 1b and 1c.

In case of small depolarization ($p \ll 1$) the depolarization ratios $\gamma_{a,b,c}$ for schemes in Fig.1a,b,c can be derived analytically [7] and are given by

4

$$\gamma_a = \frac{A_1}{\pi^2} p^2 \approx 0.014 p^2$$

$$\gamma_b = \frac{8 A_2}{\pi^4} [2a^2 + \sin^4(\frac{\pi}{8})] \cdot p^4 \approx 0.85 \cdot 10^{-4} p^4 \qquad (4)$$

$$\gamma_c = \frac{16 a^2 A_2}{\pi^4} \cdot p^4 \approx 1.07 \cdot 10^{-5} p^4$$

where

$$A_1 = \int_0^\infty \left(\frac{1}{y} - \frac{\exp(-y)}{y} - 1 \right)^2 \frac{dy}{\exp y} \cong 0.137 \qquad A_2 = \int_0^\infty \left(\frac{1}{y} - \frac{\exp(-y)}{y} - 1 \right)^4 \frac{dy}{\exp y} \cong 0.042$$

$$a = \frac{\pi}{8} - \frac{1}{4} - \frac{\sin^2(\pi/8)}{\sqrt{2}} \qquad (5)$$

In order to check these theoretical predictions, we performed the following experiments. The second harmonic (λ=532nm) of a continuous wave Nd:YAG laser with power up to 5.5 W was used as the laser source. The Gaussian beam at the $1/e^2$ intensity was measured to be 2 mm in diameter (although our results are independent of beam waist). A laser beam was transmitted through the Faraday isolator only in one direction - from right to left (Fig. 1). To allow for direct comparisons, we used the same two magneto-optical elements in each isolation experiment. The magnetic field was chosen such that the total angle of rotation was equal to 45°. The optical elements were made from magneto-optical glass 17 mm in diameter. Absorption at 532 nm was measured to be 0.05 cm^{-1} taking into account reflective losses. In addition, we used relatively weak magnetic fields and long optical elements (52 mm and 68 mm, respectively) to obtain large values of the parameter p at low laser powers. The first element in the optical path of the laser beam was chosen to be shorter than the other, thus allowing us to have approximately equal values of absorbed power P_h and, consequently, of the parameter p in the both elements.

5

In order to define the value of parameter p in the experiment, it was necessary to measure the ratio Q/κ for the magneto-optical glass. The laser beam was transmitted through the magneto-optical element placed between a pair of crossed polarizers without any magnetic field. The depolarization ratio $\gamma(H=0)$ was measured as a function of p. The measured dependence was in good agreement with the theoretical formula [6,7].

$$\gamma(H=0) = 0.017 \left[\frac{P_h Q}{\lambda \kappa} \right]^2 = 0.017 p^2 \tag{6}$$

The value of P_h was measured experimentally while the ratio Q/κ was used as a fitting parameter. The best fit gave a value of $Q/\kappa = 1.2 \times 10^{-6}$ m/W. We performed these measurements for both rotators used in our experiments. In principle, they should give the same results because of parameter Q/κ characterizes the magneto-optical medium itself and does not depend on the length of the optical element. Indeed, the difference between these two measurements was 2%. To check the accuracy of this measurement technique, the parameter Q/κ was measured for some optical glasses for which the ratio was known from literature. The disagreement with the known from literature data was no more than 15%.

Figure 2 shows the dependencies of $\gamma(p)$ for each isolation method. The solid lines indicate the results of theoretical analysis [7] made for the photoelastic effect neglecting temperature dependence of Verde constant. The disagreement between the theoretical predictions and experimental data at low power is due to the residual, power independent depolarization in magneto-optical elements. This depolarization is due to linear birefringence induced by intrinsic stresses in the optical elements. In general, these stresses have random nature and are different in the two elements and is not included in our model.

However, there is some correlation between them due to the shape dependence of the stress resulting from mechanical surface processing. However, the nature of the linear birefringence does not matter for depolarization compensation. If the optical elements have the same birefringence, the depolarization is compensated using the methods shown in Fig1b,c. It is also true that if the optical elements have similar (but not the same) birefringence the depolarization is only compensated partially. The more correlated the birefringence in the optical elements are, the more efficient the compensation will be. Thus at low powers, the residual depolarization seen in curves b,c of Fig.2 is greater than the theoretical prediction. Nevertheless, each modified geometry produces an isolation ratio better than the traditional method shown in curve a of Figure 2.

When the power is increased, the self-induced depolarization competes with residual depolarization and, at high powers, the depolarization ratio is mainly determined by self-induced effects, where experimental data are in good agreement with theoretical predictions for all three geometries (see Fig.2). For the traditional geometry, the power at which residual depolarization may be neglected is relatively small ($\log p$=-0.3). In on the method used for Fig.1b, this power is much greater ($\log p$=0.5) due to suppression of self-induced depolarization. In the method displayed in Fig.1c, the self-induced depolarization is compensated even more efficiently and the power where self-induced effects dominate is approximately $\log p$=0.8. Such high power was not available in our experiments. This explains the disagreement between theory and experiment for the geometry shown in Fig.1c. Even at maximum laser power, the theoretical value of γ is less than 0.002, which is comparable with the residual depolarization.

It is clear that the depolarization induced by the temperature dependence of the Verdet constant in the given schemes is not compensated and is equal for all three schemes. The good agreement of the experiment with theoretical analysis, which assumes only photoelastic-induced depolarization, shows that influence of temperature dependence of Verdet constant on depolarization ratio may be neglected. It confirms the theoretical prediction that the photoelastic effect limits the isolation ratio for Faraday isolators at high average power.

Analysis of the transverse structure of the depolarized radiation also confirms our predictions. For traditional isolation methods, the depolarized laser beam has a "dark cross" spatial profile, inclined relative to the polarization of the input field at an angle 22.5° (shown in Fig. 3a). This fully corresponds to the theoretical predictions in ref [6,7]. The dependence of the local depolarization ratio on the polar angle had a period of 90°, and the ratio of maximum to minimum is very large. It is evident that the temperature dependence of the Verdet constant should have led to a uniform over the polar angle distribution of the depolarization field. Our analysis [7] predicts a 45° period of the dependence of the local depolarization ratio for the polar angle in the geometry shown in Fig. 1b, and a uniform angular distribution in the configuration shown in Fig. 1c. Both these facts qualitatively agree with the experimental results as shown in Fig. 3b,c.

Using these results, we can estimate the maximum power of laser radiation at which the best Faraday isolation method (Fig. 1c) ensures a high depolarization ratio. For Faraday isolators at a wavelength of 1 μm, the characteristic length of optical elements is 4 cm and the absorption coefficient is 2×10^{-3} cm^{-1}. Although the value $Q/\kappa = 1.2 \times 10^{-6}$ m/W was

measured at a wavelength 532 nm and only for one type of magneto-optical glass, we use it here as a reasonable estimate for 1.064 μm. Then, from eq. (2), p is approximately equal to 1 at a laser power of 100 W. Using these values, it is evident from Fig. 2 that the optimal configuration (Fig. 1c) allows for the construction of a Faraday isolator with depolarization ratio 25-30 dB at laser power of 300-400 W. In contrast, the isolation ratio using the traditional method is less than 10 dB.

Our experimental investigation allows us to draw the following general conclusions. First, the isolation ratio of Faraday isolators at high average power is determined by the photoelastic effect rather than by the temperature dependence of the Verdet constant. In addition, the depolarization ratio in the dual-glass-based isolation methods demonstrated here is significantly lower than in the traditional method. The geometry shown in Fig. 1c is most optimal, reducing the depolarization ratio by two orders of magnitude with respect to the single isolator method. These experimental results confirm the possibility of designing a Faraday isolator based on glass magneto-optical elements with isolation of 30 dB at average laser power of hundreds of watts. Such isolators will be useful in applications such as gravitational wave interferometry [11-14] which require both high power lasers and high isolation ratios.

References

1. R. J. Shine, A. J. Alfrey, and R. L. Byer, "40-W CW, TEM$_{00}$-Mode, Diode-Laser-Pumped, Nd-Yag Miniature-Slab Laser", Opt. Lett. **20**, 459-461 (1995).

2. S. A. Payne, R. J. Beach, C. Bibeau, C. A. Ebbers, M. A. Emanuel, E. C. Honea, C. D. Marshall, R. H. Page, K. I. Schaffers, J. A. Skidmore, S. B. Sutton, and W. F. Krupke "Diode Arrays, Crystals, and Thermal Management for Solid-State Lasers" IEEE J. Sel. Top. Qaunt. **3**, 71-81 (1997).

3. A.N.Malshakov, G.A.Pasmanik, and A.K.Potemkin "Comparative characteristics of magneto-optical materials" Appl. Opt. **36**, 6403-6410 (1997).

4. N.P.Barnes and L.P.Petway. "Variation of the Verdet Constant with Temperature of Terbium Gallium Garnet" J. Opt. Soc. Am B, **9**, 1912-1915 (1992).

5. J.D.Foster and L.M.Osterink. "Thermal Effects in a Nd:YAG Laser", J. Appl. Phys. **41**, 3656-3663 (1970).

6. E.Khazanov, O.Kulagin, S.Yoshida, D.Tanner, and D.Reitze, "Investigation of Self-Induced Depolarization of Laser Radiation in Terbium Gallium Garnet" IEEE J. Quant. Electron. **35**, 1116-1122 (1999).

7. E.A. Khazanov, "Compensation of Thermally Induced Polarization Distortions in Faraday isolators", Quantum Electronics **29**, 59-64, (1999). [Kvantovaya electronika, **26**, 59-64 1999].

8. K. Shiraishi, F.Tajima, and S.Kawakami, "Compact Faraday Rotator for an Optical Isolator Using Magnets Arranged With Alternating Polarities" Opt. Lett., **11**, 82-84

(1986).

9. W.A.Clarkson, N.S.Felgate, and D.C.Hanna, "Simple method for reducing depolarization loss resulting from thermally induced birefringence in solid-state lasers". Opt.Lett. **24**, 820-822 (1999).

10. A.V. Mezenov, L.N.Soms, and A.I.Stepanov, "Thermooptics of solid-state lasers", Leningrad, Mashinostroenie, p.44 (1986).

11. A. Abramovici, W. E. Althouse, R. W. P. Drever, Y. Gursel, S. Kawamura, F. J. Raab, D. Shoemaker, L. Sievers, R. E. Spero, K. S. Thorne, R. E. Vogt, R. Weiss, S. E. Whitcomb, and M. E. Zucker, "LIGO - The Laser-Interferometer-Gravitational-Wave-Observatory" Science **256**, 325-333 (1992).

12. A. Giazotto, "Wide-band measurement of gravitational-waves - the Virgo Project", Nuovo Cimento C **15** 955-971 (1992).

13. M. V. Plissi, K. A. Strain, C. I. Torrie, N. A. Robertson, S. Killbourn, S.Rowan, S. M. Twyford, H. Ward, K. D. Skeldon, and J. Hough, "Aspects of the suspension system for GEO 600" Rev. Sci. Instrum.**69**, 3055-3061 (1998).

14. K. Kawabe, "Status of TAMA project", Classical and Quantum Grav. **14**, 1477-1480 (1997).

Figure captions

Fig. 1. (a) Traditional method for Faraday isolation and novel [7] geometries (b) with a $\lambda/2$ plate and (c) with a reciprocal rotator. 1,4 - polarizers; 2,6 - $\lambda/2$ plates; 3 - 45° Faraday rotator; 5 - 22.5^o clockwise Faraday rotator; 7 - 22.5^o counterclockwise Faraday rotator; 8 - 67.5^o reciprocal polarization rotator.

Fig.2. Power dependence of $\gamma(p)$ for the geometries shown in Fig.1a (a, circles), Fig.1b (b, triangles) Fig.1c (c, squares). The depolarization is suppressed almost two orders of magnitude at high powers when using the Faraday isolator geometries shown in Fig. 1b,c.

Fig.3 Images of the spatial profiles of the depolarized beams after transmission through the isolators for each geometry shown in Fig.1a (a), Fig.1b (b) Fig.1c (c).
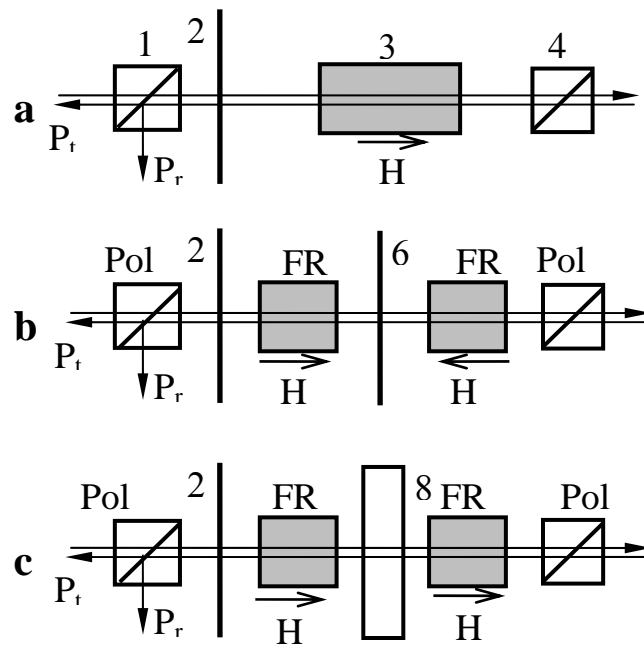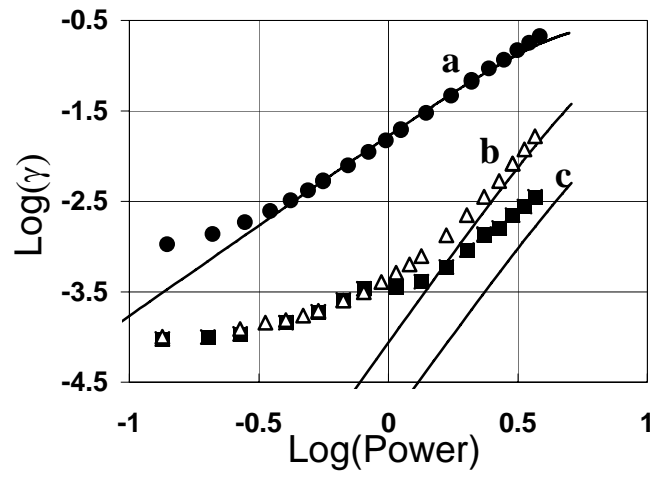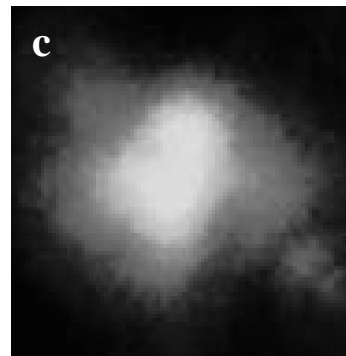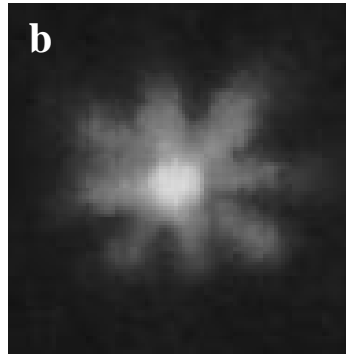
a

1   2   3   4

P_t P_r H

b

Pol   2   FR   6   FR   Pol

P_t P_r H   H

c

Pol   2   FR   8 FR   Pol

P_t P_r H   H

Fig.1.

Fig.2

Fig.3.